

## Article

# Thermal and Tribological Properties Enhancement of PVE Lubricant Modified with SiO<sub>2</sub> and TiO<sub>2</sub> Nanoparticles Additive

Mohd Farid Ismail <sup>1</sup>, Wan Hamzah Azmi <sup>2,3,\*</sup>, Rizalman Mamat <sup>3</sup> and Hafiz Muhammad Ali <sup>4,\*</sup>

<sup>1</sup> Faculty of Mechanical and Manufacturing Engineering Technology, Universiti Teknikal Malaysia Melaka, Hang Tuah Jaya, Durian Tunggal 75150, Melaka, Malaysia

<sup>2</sup> Centre for Research in Advanced Fluid and Processes, Lebuhraya Tun Razak, Gambang, Kuantan 26300, Pahang, Malaysia

<sup>3</sup> Faculty of Mechanical and Automotive Engineering Technology, Universiti Malaysia Pahang, Pekan 26600, Pahang, Malaysia

<sup>4</sup> Mechanical Engineering Department, King Fahd University of Petroleum and Minerals, Dhahran 31261, Saudi Arabia

\* Correspondence: wanazmi2010@gmail.com (W.H.A.); hafiz.ali@kfupm.edu.sa (H.M.A.)

**Abstract:** The addition of nanoparticles may have a positive or negative impact on the thermal and tribological properties of base lubricant. The objective of this paper is to investigate the effect of nanoparticle dispersion in lubricant base in relation to its application in refrigeration system compressors. An investigation of tribological and thermal properties of nanolubricants for rolling piston rotary systems was carried out through four-ball tribology tests and thermal conductivity measurements. Nanolubricants dispersed with SiO<sub>2</sub> and TiO<sub>2</sub> nanoparticles were tested at various concentrations and temperatures. The changes in thermal conductivity and coefficient of friction (COF) were analyzed while wear weight loss was also calculated from wear scar size. A regression model of thermal conductivity enhancement was proposed for both types of nanoparticles. Zeta potential results show that nanolubricants have excellent stability. The thermal conductivity increases by the increment of nanoparticle concentration but decreases by temperature. The R-square for the regression model is more than 0.9952 with an average deviation not more than 0.29%. The COF for SiO<sub>2</sub>/PVE nanolubricant at 0.003 vol.% reduced 15% from the baseline. The COF for nanolubricants exceeds the result for base lubricants when the concentration is more than the threshold value. The optimum concentration of SiO<sub>2</sub> and TiO<sub>2</sub> nanoparticles improved the thermal and tribological properties of PVE lubricant and may offer an advantage when applied to refrigeration systems.



**Citation:** Ismail, M.F.; Azmi, W.H.; Mamat, R.; Ali, H.M. Thermal and Tribological Properties Enhancement of PVE Lubricant Modified with SiO<sub>2</sub> and TiO<sub>2</sub> Nanoparticles Additive. *Nanomaterials* **2023**, *13*, 42. <https://doi.org/10.3390/nano13010042>

Academic Editor: Christophe Donnet

Received: 14 November 2022

Revised: 29 November 2022

Accepted: 18 December 2022

Published: 22 December 2022



**Copyright:** © 2022 by the authors. Licensee MDPI, Basel, Switzerland. This article is an open access article distributed under the terms and conditions of the Creative Commons Attribution (CC BY) license (<https://creativecommons.org/licenses/by/> 4.0/).

## 1. Introduction

Moving parts and interacting surfaces in mechanical motion may produce heat during the operation. Continuously scrubbing the surface may cause long-term harm to the component [1]. As a preventative measure, lubricants are introduced into the mechanical system to reduce friction and heat. The use of a lubricant in a mechanical system helps to save energy and prolong the component's lifespan [2]. Therefore, lubricants are important to use for a variety of purposes, including cooling, sealing, and lubricating. In a vapor compression refrigeration (VCR) system, lubricant in the compressor works at high temperature and pressure. Typically, extreme pressure and anti-wear additives are used to enhance a fluid lubricant's tribological performance by minimizing friction and surface degradation under harsh circumstances [3]. As most energies are consumed by the compressor, heat and tribological properties play an important role in determining the total energy consumption of the system.

The enhanced efficiency of machinery and equipment is one of the pillars of the global commitment to energy and environmental conservation. After the oil price shock of the 1970s, the demand for efficient and lower power-usage equipment rose as the price per unit of energy progressively increased [4]. As a result, the demand for high-efficiency appliances grew. Manufacturers, researchers, and other industrial players consistently work hard to fulfil the need of society for more environmentally friendly machines. The efficiency of an appliance can be improved through the introduction of high-efficiency components [5]. For instance, the efficiency of air conditioning can be improved by enhancing the operating components such as heat exchangers or compressors. However, changing component design is costly and time consuming. Therefore, nanoparticle dispersion technology was introduced to enhance system performance without replacing the existing components [6].

Nanoparticle dispersion technology is the method of dispersing less than 100 nm nanoparticles in a base fluid commercially known as a nanofluid [7]. The introduction of nanofluids to mechanical components has shown promising results for highly efficient systems [8]. The application of nanofluids in refrigeration systems was initiated by Wang et al. [9]. TiO<sub>2</sub> nanoparticles were dispersed in a mineral oil base and the newly invented oil was named a nanolubricant. Then, the nanolubricant was applied to a R134a refrigerating system for performance measurement study. This experiment showed that the nanolubricant can improve the compatibility of lubricant with hydrofluorocarbon (HFC) refrigerant. Later, more studies were conducted related to the application of nanolubricant in refrigeration systems such as domestic refrigerators, heat pumps, air conditioning and chiller systems [10–12]. The nanolubricant studies also included the research in automotive air conditioning systems that was pioneered by Sharif et al. [13]. Base lubricants such as mineral oil (MO), polyol ester (POE), or polyethylene glycol (PAG) are commonly used for nanolubricant studies due to their solubility with the specific type of refrigerant. Meanwhile, the refrigerant is selected depending on its operating properties that fulfil the need of refrigerating system. Operating pressure, ambient temperature and type of compressor are amongst the primary factors that determine the selection of suitable refrigerant for a refrigeration system.

The initial research into nanolubricants focused on the physical properties of the fluid. The change of viscosity, thermal conductivity, and density of the lubricants was studied. Subsequently, tests for tribological properties were also undertaken in the research, as a response to the need to understand the friction effect of nanoparticles on the contact surfaces. The importance of the thermal conductivity property of nanofluids is undeniable since the pioneering research in nanoparticle dispersion technology [14,15]. In a refrigerant-nanolubricant mixture system, thermal conductivity always becomes one of the most important properties to be studied [16,17]. The presence of nanoparticles in the nanolubricant always positively impacts the performance of the VCR system as thermal conductivity values increase by the increment of nanoparticle concentration [18,19]. Some researchers combined the study on thermal conductivity with tribology [20–22]. As the tribological property increased the system's ability to reduce friction in mechanical movement, thermal conductivity increases the system's capacity to transfer heat efficiently [23]. Nanoparticle dispersion in lubricant has already been proven by some researchers as being able to increase the performance and reduce the energy consumption of a mechanical system [24]. Nanoparticles acted as a roller between two contact surfaces thus reducing the frictional effect. However, the volume concentration of nanoparticles must not exceed a threshold value. Values over this limit may cause tribological behavior to show lower improvement [25].

A relatively new compressor lubricant for the VCR system, polyvinyl ether (PVE), is considered to be a favorable alternative to POE oil. Unlike POE and PAG, the PVE oil does not hydrolyze water. Therefore, hydrolysis is not required in a system, especially useful in the VCR system. The filter dryer can be eliminated, and the long vacuuming process also can be shortened. Being a constituent of polymer base oil also brings advantages as the PVE retains its characteristics despite changes in viscosity [26]. However, studies

on the properties of PVE are still lacking. Furthermore, nanolubricant research with PVE as lubricant base is far behind. Motozawa et al. [27] is the only report available of PVE nanolubricant with CuO as additive. The properties studied were thermal conductivity, viscosity, and dielectric constant. As far as the authors are aware, no report has been published to date on the tribological property of PVE nanolubricants. PVE's role as a lubricant was previously intended as compressor lubricant in air conditioning systems. In such applications, tribological, thermal, and rheological properties of lubricant play an important role in determining the performance of such a system. However, the pure PVE lubricant is reasonably low in thermal conductivity and viscosity [28]. Nanoparticle additives solve this issue by increasing the thermal conductivity as well as improving the tribological property of lubricant [29,30]. SiO<sub>2</sub> and TiO<sub>2</sub> nanoparticles were amongst the best nanoparticle candidates able to improve the performance of VCR system [31,32]. In this study, the thermal and tribological properties of PVE nanolubricant will be investigated. The SiO<sub>2</sub> and TiO<sub>2</sub> nanoparticles will be used as an additive to discover the improvement in thermal and friction properties.

## 2. Experimental Methods

### 2.1. Nanolubricant Preparation and Stability Evaluation

The PVE lubricant used in this paper was procured from Idemitsu Kosan Co., Ltd. This lubricant is commonly used for HFC refrigeration compressors, especially for residential air conditioning systems. Table 1 summarizes the chemical-physical properties of PVE lubricant. The 99.9% purity SiO<sub>2</sub> nanoparticle used in this paper was obtained from HWNANO (Hongwu International Group Ltd., Guangzhou, China), while the TiO<sub>2</sub> nanoparticle was from DKNANO (Beijing Deke Daojin Science and Technology Co., Ltd., Beijing, China) and also has the same purity percentage. Table 2 summarizes the properties of nanoparticles used in this paper. The SiO<sub>2</sub> and TiO<sub>2</sub> nanolubricant in this paper were prepared using a two-step method. The measurement of nanoparticles for different volume concentrations is calculated using Equation (1)

$$\phi = \frac{\frac{m_n}{\rho_n}}{\frac{m_n}{\rho_n} + \frac{m_l}{\rho_l}} \times 100\% \quad (1)$$

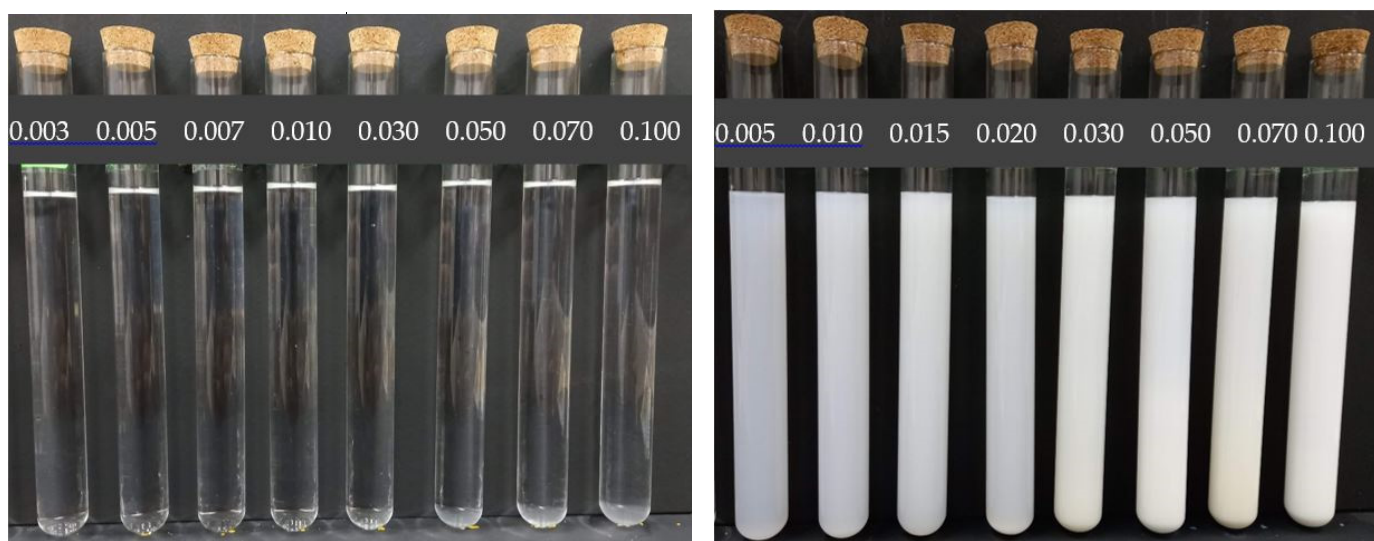
where  $\phi$  is the concentration in volume percent,  $m_l$  and  $m_n$  are the masses of PVE lubricant and nanoparticle, respectively, while  $\rho_l$  and  $\rho_n$  are the density of PVE lubricant and nanoparticle, respectively. Nanoparticles were weighed using a high precision ( $\pm 0.0001$ ) weighing scale. The minimum volume of each concentration prepared was 100 mL. The nanoparticles were poured into stirred lubricant very gradually to avoid agglomeration. The stirring process took half an hour before the nanolubricants were transferred to the homogenizing process [33]. The homogenizer equipment used in this study was an ultrasonic water bath (Fisherbrand FB15051) with 200W power and 50 kHz constant frequency. The homogenizing process took 1 h for SiO<sub>2</sub> and 5 h for TiO<sub>2</sub> nanolubricants. Figure 1 shows part of the prepared sample of both types of nanolubricants. The photos for visual stability evaluation were captured just after nanolubricant preparation was completed. The stability of nanolubricants was also measured by using the zeta potential method as suggested by [34]. 5 mL of sample from a 0.01% concentration of both type nanolubricants were separated from the main beaker for this purpose. As the concentration is not a factor that determines the zeta potential measurement, only one concentration was tested that represents the stability of all nanolubricants. The zeta potential measurement was repeated three times for each sample and the average value was calculated and is presented. To characterize and identify of nanolubricants, a small amount of the samples was sent to the laboratory for microscopy evaluation. A TECNAI G2 F20 X-Twin high-resolution transmission electron microscope (HRTEM) was used in this study to ensure the presentation, size, shape, and position of the nanoparticles in the prepared sample.

**Table 1.** Properties of base lubricant: [26].

Property	PVE
Dynamic Viscosity, mm <sup>2</sup> /s @ 40 °C	68.1
Dynamic Viscosity, mm <sup>2</sup> /s @ 100 °C	8.04
Viscosity index	84
Pour Point, °C	-37.5
Flash point, °C	204
Density, kg/m <sup>3</sup> @ 15 °C	936.9

**Table 2.** Properties of nanoparticles [35,36].

Property	Nanoparticles	
	SiO <sub>2</sub>	TiO <sub>2</sub>
Density, $\rho$ [kg/m <sup>3</sup> ]	2220	4230
Thermal conductivity, $k$ [W/mK]	4	8.4
Molecular mass, $M$ [g/mol]	60.08	79.87
Average diameter, $d_p$ [nm]	15	30–50
Specific surface area [m <sup>2</sup> /g]	250	-
Specific heat, $c_p$ [J/kgK]	745	692

(a) SiO<sub>2</sub>/PVE(b) TiO<sub>2</sub>/PVE**Figure 1.** Nanolubricants after preparation at different volume concentration (%).

The SiO<sub>2</sub>/PVE nanolubricants were prepared at concentrations from 0.003% to 0.1% while TiO<sub>2</sub>/PVE nanolubricants were from 0.005% to 0.1%. For thermal property measurement, the minimum concentration was conducted at 0.01% for both types of nanolubricants. The limited measurement capability of thermal conductivity devices does not allow lower concentrations to be tested as the deviation of thermal conductivity is too small compared to the measurement error. For tribological measurement, the tests were conducted starting from the 0.003% and 0.005% concentrations for SiO<sub>2</sub>/PVE and TiO<sub>2</sub>/PVE nanolubricant, respectively.

## 2.2. Thermal Conductivity Measurement

The thermal conductivity measurement was conducted using TCi Thermal Conductivity Analyzer by C-Therm. It has less than 5% accuracy for the measurement range between 0 to 500 W/mK. The samples were measured between 30 to 80 °C. A 35 mL sample was filled

in a sample cell. The thermal sensor was connected and located properly in the dedicated oven. The heat imposed on the sample and thermal effusivity was measured. The thermal conductivity was calculated from the effusivity measurement together with heat capacity and density as input. The device recorded one thermal conductivity value for every 0.2 °C increment. This method used in this thermal conductivity measurement applied Modified Transient Plane Source (MTPS) that conforms to ASTM D7984. The measurement for each nanolubricant was repeated three times to confirm the repeatability of measurement, and the average value was taken as final experimental data. The thermal conductivity models by Hamilton and Crosser [37], Redhwan et al. [18], and Zawawi et al. [19] shown in Table 3 are used to verify the thermal conductivity of SiO<sub>2</sub>-TiO<sub>2</sub>/PVE nanolubricants.

**Table 3.** Thermal conductivity model.

Models	Correlations
Hamilton and Crosser [37]	$k_r = \frac{k_{eff}}{k_{bf}} = \frac{k_p + (n-1)k_{bf} - (n-1)\varphi(k_{bf} + k_p)}{k_p + (n-1)k_{bf} + \varphi(k_{bf} + k_p)}$
Redhwan et al. [18]	$k_r = \frac{k_{eff}}{k_{bf}} = 1.2 \left(1 + \frac{\phi}{100}\right)^{0.04} \left(1 + \frac{T-273}{80}\right)^{-0.01}$
Zawawi et al. [19]	$k_r = \frac{k_{eff}}{k_{bf}} = \left(1 + \frac{\phi}{100}\right)^{9.8} \left(1 + \frac{T-273}{80}\right)^{0.002}$

### 2.3. Tribology Measurement

The tribological properties investigation was carried out using the Koehler Four-Ball Tribometer for PVE base lubricant and nanolubricant with SiO<sub>2</sub> and TiO<sub>2</sub> nanoparticles additive. This method was also extensively used by Sanukrishna et al. [23], Kamel et al. [3], and Wang and Wang [38] for nanolubricant studies with different lubricant bases and additives. The relative investigation was carried out according to ASTM D4172. The steel balls are chromium steel ball G20 that are manufactured in accordance with the ISO 3290 protocol. Hexane was used to clean the balls and tools from any oil or debris. Three balls were located inside the oil handler and tightened. The lubricant submerged the balls and the contact surface touched the fourth ball from the top. A load of 40 Nm was applied to the balls while the rotating speed was set at 1200 rpm. A thermocouple was connected to the oil handler to measure the lubricant temperature. A heater with an automatic temperature controller was used to maintain the lubricant temperature at 75 °C. The equipment and set up for the tribological testing conducted in the current study is presented in Figure 2.

Wear scar morphology is one of the methods that can be used to evaluate the anti-wear characteristics of lubricants. The wear scar diameter (WSD) provides information about friction load capacity and the severity of wear due to friction. Greater wear rate can be determined by the bigger size of WSD and vice versa. The wear weight loss ( $W_{loss}$ ) can be determined using Equations (2) to (4)

$$W_{loss} = W_{int} - W_{final} \quad (2)$$

$$W_{loss} = \frac{1}{3} \pi h_l^2 \left( \frac{3}{2} D - h_l \right) \quad (3)$$

$$h_l = \frac{D}{2} - \sqrt{\left(\frac{D}{2}\right)^2 - \left(\frac{d}{2}\right)^2} \quad (4)$$

where  $W_{int}$  in grams (g) is the initial weight of the ball before the test;  $W_{final}$  in grams (g) is the final ball weight after the test;  $D$  is the diameter of the ball which is 12.7 mm;  $d$  is the diameter of wear scar in mm and  $h_l$  is the height of loss volume. The weight of each ball was measured using a high-accuracy weighing scale and recorded for volume loss calculation later.

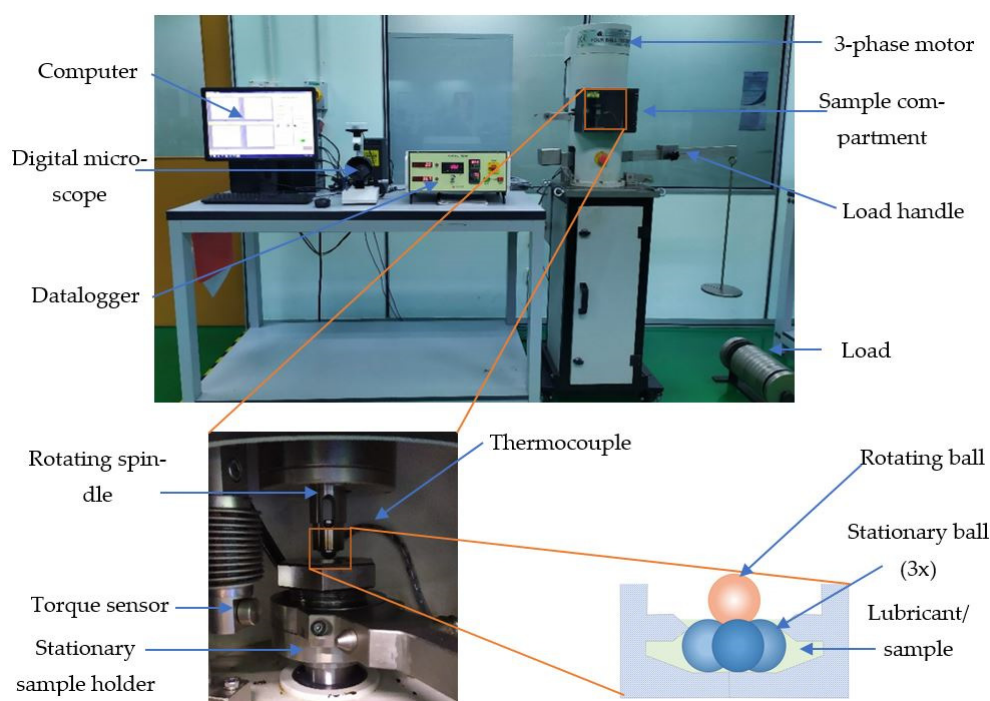


**Figure 2.** Four-ball Tribology Testing Machine.

#### 2.4. Uncertainty Analysis

The uncertainties for the thermal conductivity analyzer and four-ball tribology tester are presented in Table 4. The uncertainties of measurement are analyzed with less than 1.09%.

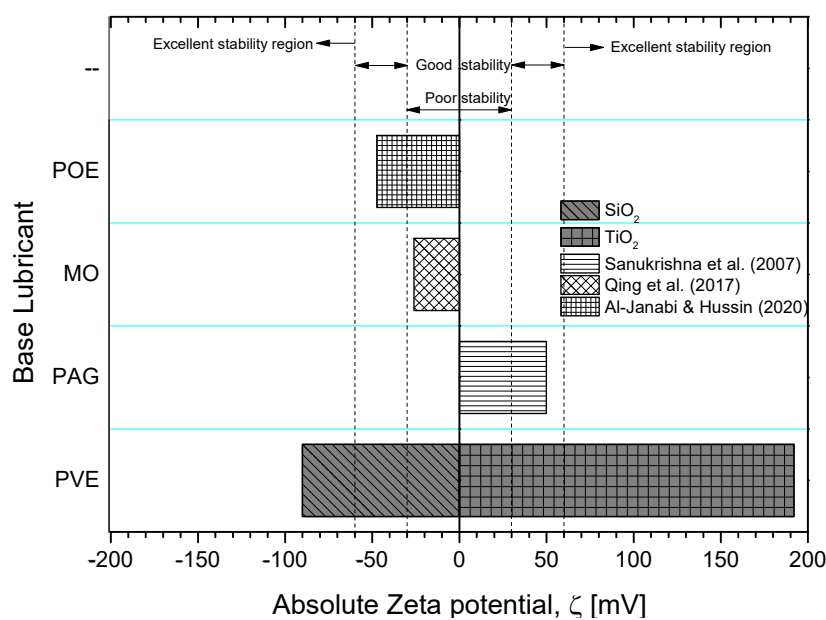
**Table 4.** The summary for the uncertainty.

Parameters	Accuracy	Values Measured		Uncertainty (%)
		Min	Max	
Thermal conductivity, $k$ [W/mK]	$\pm 0.001$	0.136	0.148	0.67–0.73
Coefficient of friction, <i>COF</i>	$\pm 0.001$	0.091	0.139	0.72–1.09

### 3. Results and Discussion

#### 3.1. Stability of Nanolubricants

Visual observation of the prepared nanolubricants showed that the  $\text{SiO}_2/\text{PVE}$  and  $\text{TiO}_2/\text{PVE}$  nanolubricants were stable for up to 30 days. No separation occurred between lubricant and nanoparticles. However, a small amount of sedimentation was observed at the bottom of the nanolubricant showing that there was some gravitational effect on the dispersed nanoparticles. The initial murky white nanolubricants became clearer 30 days after the preparation. The zeta potential test on one sample of each type of nanolubricant was conducted on the same day as preparation. The results are shown in Figure 3 [39–41].  $\text{SiO}_2/\text{PVE}$  nanolubricant returned a zeta potential value of  $-90 \text{ mV}$  while  $\text{TiO}_2/\text{PVE}$  was  $192 \text{ mV}$ . According to Ghadimi et al. [42], a zeta potential of more than  $60 \text{ mV}$  is considered to have excellent stability. The same figure also compares to the zeta potential value from literature with different lubricant bases [39–41]. Based on the visual observation and zeta potential test on the nanolubricants, both types of nanolubricants have excellent stability up to 30 days.



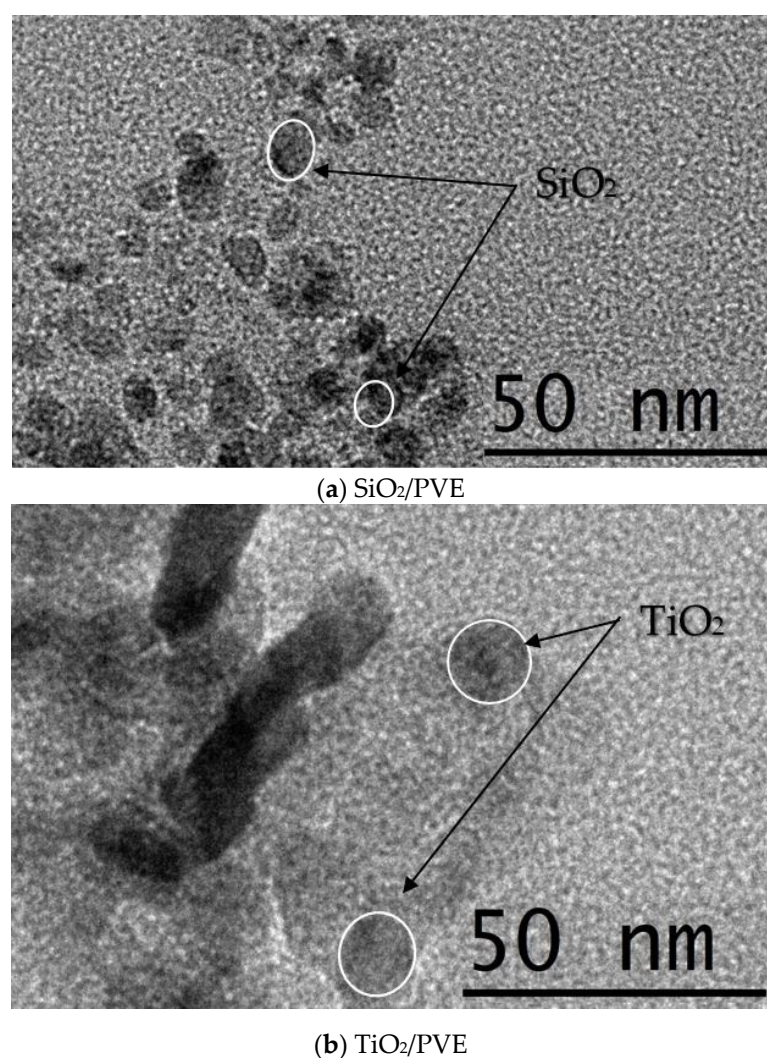
**Figure 3.** Zeta Potential measurement comparison of present study nanolubricant with literature [39–41].

Figure 4 shows the results of the HRTEM image captured from the prepared nanolubricants. The image was captured with a resolution of  $\times 88,000$  so that the size of the nanoparticle dispersed in PVE lubricant was able to be determined. The image confirmed the average size of  $\text{SiO}_2$  nanoparticles as 15 nm while the  $\text{TiO}_2$  was 30 nm. The nanoparticles in the lubricant base were uniformly distributed with some agglomeration present.

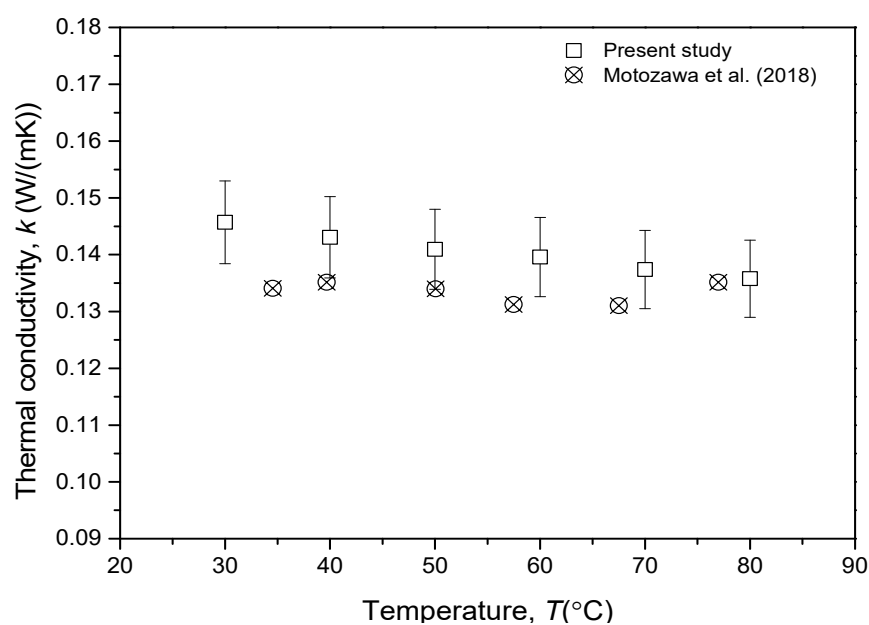
### 3.2. Thermal Conductivity of Nanolubricants

Figure 5 depicts the comparison of thermal conductivity measurement of pure PVE lubricant in the present study with available references from the literature. The comparison was made as a verification of the current thermal conductivity measurement with the report from previous findings by Motozawa et al. [27]. Even though the PVE lubricant used in this current study was not the same as their PVE lubricant, in that they were of different manufacturers, both lubricants were of the same grade. The comparison was made at environment temperatures between 30 and 80 °C. The results showed that the present thermal conductivity measurements were within a 5% deviation from the measurement made by Motozawa et al. [27]. The results also revealed that the thermal conductivity of pure PVE lubricant was slightly decreased by the increment of temperature.

The thermal conductivity measurement of  $\text{SiO}_2$  and  $\text{TiO}_2$  nanolubricant also shows a similar trend to pure PVE lubricant. Figure 6a,b present the thermal conductivity measurement and its enhancement for both types of nanolubricants, respectively. The thermal conductivity of pure PVE was also plotted as a comparison to the measurement for nanolubricants. The results indicated that nanolubricants had higher thermal conductivity than pure PVE lubricants at all measured temperatures. However, the value of thermal conductivity decreased when the temperature increased. At 30 °C, the thermal conductivity was the highest. The results also revealed that  $\text{TiO}_2$ /PVE nanolubricants always had higher thermal conductivity than that of  $\text{SiO}_2$ /PVE at the same concentration. The  $\text{TiO}_2$  nanoparticles had higher thermal conductivity ( $8.4 \text{ W/m}\cdot\text{K}$ ) values compared to  $\text{SiO}_2$ , which was only  $4 \text{ W/m K}$  as presented in Table 2. The thermal conductivity measurement of  $\text{SiO}_2$  and  $\text{TiO}_2$  nanolubricant also showed a similar trend for pure PVE lubricant.



**Figure 4.** TEM image of nanolubricants.



**Figure 5.** Thermal conductivity verification of PVE lubricant with available references [27].

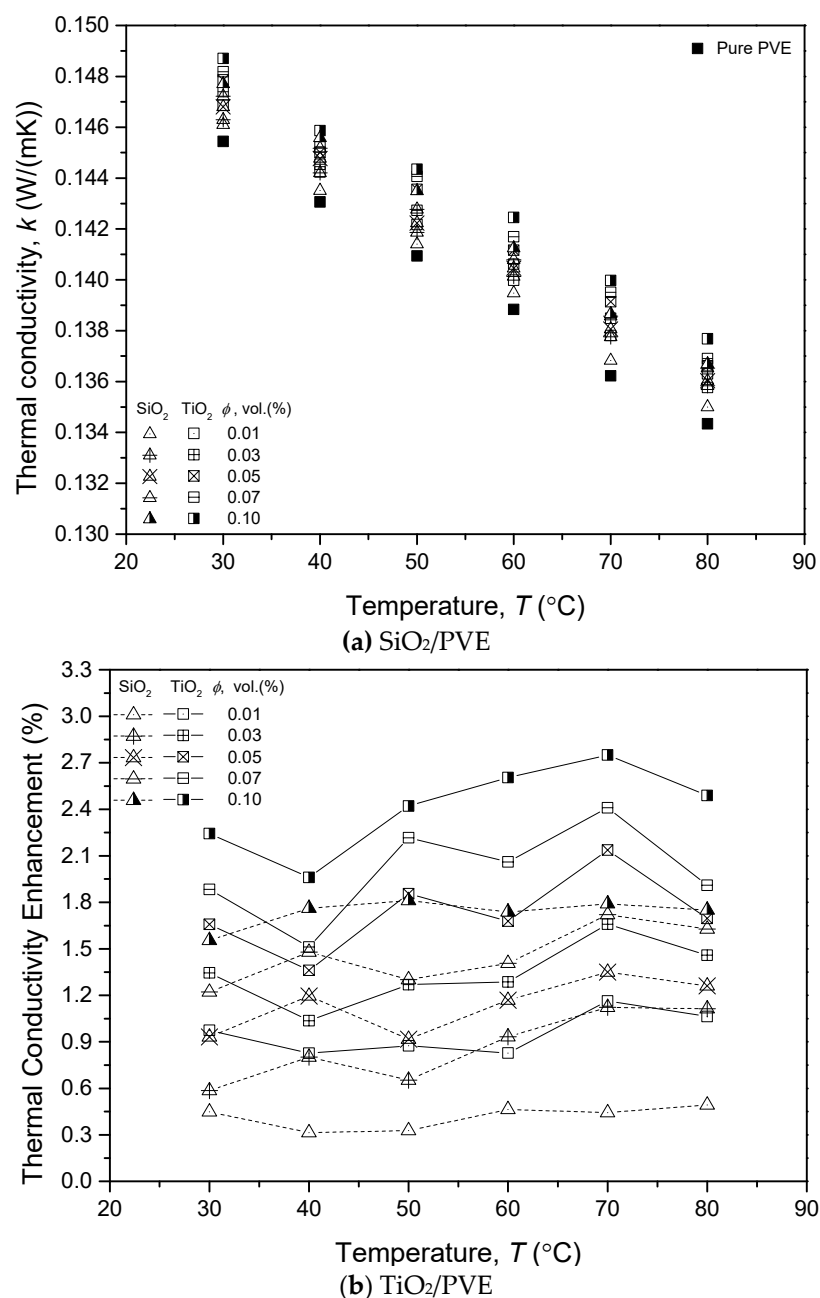


**Figure 6.** Thermal conductivity (a) measurement (b) increment for  $\text{SiO}_2/\text{PVE}$  and  $\text{TiO}_2/\text{PVE}$  nanolubricants.

The thermal conductivity of nanolubricants at all measured concentrations was always higher than that of pure PVE lubricant, as depicted in Figure 6b. The enhancement trend shows that the increment of nanoparticle concentration may increase the thermal conductivity. It was also discovered that temperature did not influence the amount of thermal conductivity increment of the nanolubricants. There was no significant trend of thermal conductivity changes when the temperature changed. The current finding was aligned with thermal conductivity enhancement reported by Sharif et al. [13] who studied the properties of PAG lubricant dispersed with  $\text{Al}_2\text{O}_3$  nanoparticle. The thermal conductivity enhancement of PVE nanolubricants was considered as insignificant as the maximum increment was less than 3%, with a volume concentration of 0.10%  $\text{TiO}_2$  nanoparticles. The presence of nanoparticles in PVE lubricant influenced the heat-conducting behavior as the nanoparticles themselves had a better capability of conducting heat. However, when

the heat was applied to the liquid, the nanoparticles and lubricant molecules started to vibrate and move apart from each other. Therefore, the thermal conductivity between nanoparticles and molecules decreased as the possibility of particle collision decreased at a higher temperature.

### 3.3. Thermal Conductivity Regression Model Analysis

From the experimental measurement results, regression analysis was performed on the thermal conductivity ratio of nanolubricant to pure PVE lubricant. Two effective thermal conductivity equations were proposed for  $\text{SiO}_2/\text{PVE}$  and  $\text{TiO}_2/\text{PVE}$  nanolubricant as presented in Equations (5) and (6), respectively. Both equations are valid for nanoparticle concentrations of  $0 \leq \phi \leq 0.1\%$  and temperatures between  $30 \leq T \leq 80^\circ\text{C}$ . Figure 7a shows the plot determining thermal conductivity using the equation model ( $k_{Model}$ ) versus the experiment data ( $k_{Exp}$ ). There was a good agreement of the regression equation with the experimental data where the deviation between those thermal conductivity values were  $\pm 1\%$ . The regression was convincing, with an  $R^2$  value for both nanolubricants of more than 0.9867. The AD was not more than 0.3%, and the SD was less than 0.2%.

$$k_r = \frac{k_{nl}}{k_l} = \frac{\left(1 + \frac{\phi}{100\%}\right)^{20}}{\left(0.1 + \frac{T}{80^\circ\text{C}}\right)^{0.001}} \quad (5)$$

$$k_r = \frac{k_{nl}}{k_l} = \frac{\left(1 + \frac{\phi}{100\%}\right)^{21}}{\left(0.1 + 1.1 \frac{T}{80^\circ\text{C}}\right)^{0.003}} \quad (6)$$

Further investigation of the regression model was conducted using the statistical method as presented in Figure 7b. The margin of deviation (MOD) of each point was calculated using Equation (7) and plotted to illustrate the size of the deviation percentage. In addition, the difference between the experimental data and the predicted model was also presented as residuals in the same figure. The distribution of MOD and residuals of nanolubricants did not exceed  $\pm 1\%$  and 0.001, respectively. The distribution of points was random without any significant trend. The ANOVA was also conducted for  $\text{SiO}_2/\text{PVE}$  and  $\text{TiO}_2/\text{PVE}$  nanolubricants regression model and presented in Table 5. It was shown that the regression model was very accurate based on the statistical analysis performed on it.

$$MOD = \left[ \frac{(k_{nl})_{Exp} - (k_{nl})_{Model}}{(k_{nl})_{Exp}} \right] \times 100\% \quad (7)$$

To ensure that the current experimental data and the regression model were correct, a comparison was made with the previously published data, as shown in Figure 8. The model suggested by Hamilton and Crosser [37] was used as the main reference in this comparison. In addition, the regression model using PAG as the base lubricant was also used as a reference, as their model was valid for the concentration studied in this research [18,19]. For a fair comparison, the temperature for all data was fixed at  $50^\circ\text{C}$ . The model and experiment data in the current study showed a significant trend with the literature, where the thermal conductivity increases with the increment of volume concentration. The thermal conductivity for nanolubricants was always higher than that of pure lubricants showing the significant impact of nanoparticle dispersion in the modified lubricant. The model proposed for both  $\text{SiO}_2/\text{PVE}$  and  $\text{TiO}_2/\text{PVE}$  nanolubricants had good agreement with the experimental data with an error of less than 0.2%.

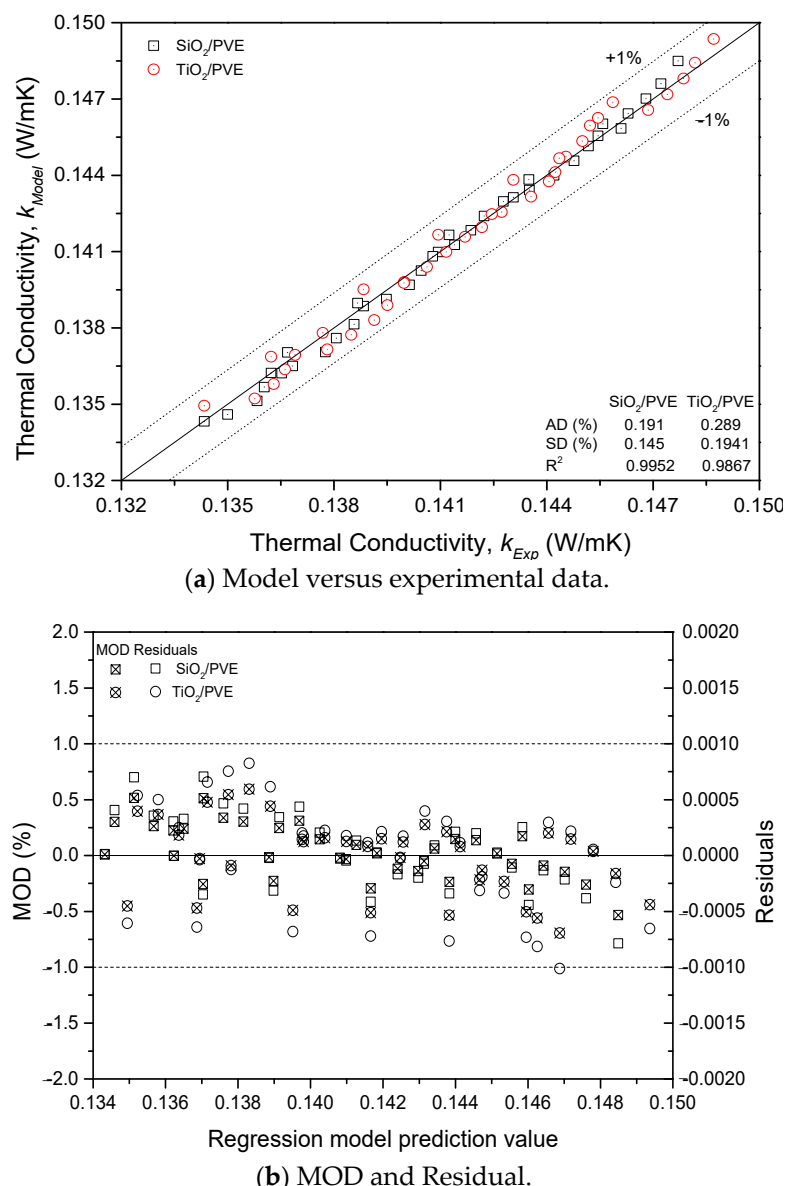


**Figure 7.** Regression model and statistical analysis of nanolubricants thermal conductivity.

**Table 5.** Analysis of variance (ANOVA) for thermal conductivity of proposed regression.

	Nanolubricant	df	SS	MS	F	Significance F
Regression	SiO <sub>2</sub> /PVE	1	0.0005762	0.00058	7059.1402	$5.07 \times 10^{-41}$
	TiO <sub>2</sub> /PVE	1	0.000584	0.000584	2520.0464	$1.77 \times 10^{-33}$
Residual	SiO <sub>2</sub> /PVE	34	$2.775 \times 10^{-6}$	$8.2 \times 10^{-8}$		
	TiO <sub>2</sub> /PVE	34	$7.879 \times 10^{-6}$	$2.32 \times 10^{-7}$		
Total	SiO <sub>2</sub> /PVE	35	0.0005789			
	TiO <sub>2</sub> /PVE	35	0.0005918			

### 3.4. Frictional Properties

The frictional property of pure PVE and its nanolubricants was evaluated by the coefficient of friction changes. The COF was calculated from the frictional torque ( $T_f$ ) in kg·cm and the normal load ( $W_N$ ) in kg applied to the balls expressed in Equation (8). The equation was obtained from the present experimental data.

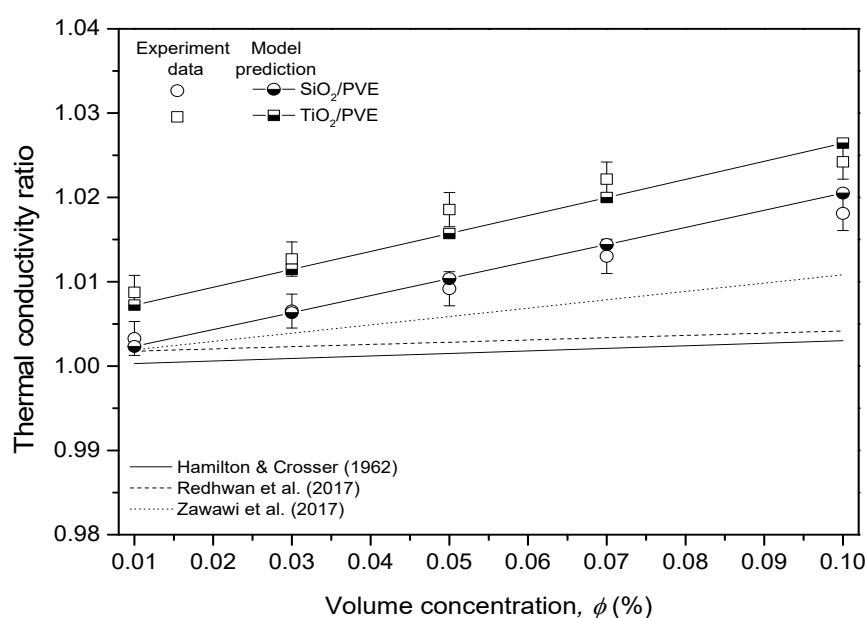


**Figure 8.** Comparison of thermal conductivity with literature and predicted model at 50 °C [18,19,37].

$$COF = 2.23004 \frac{T_f}{W_N} \quad (8)$$

Figure 9a,b illustrates the COF for  $\text{SiO}_2/\text{PVE}$  and  $\text{TiO}_2/\text{PVE}$  nanolubricants with different concentrations, respectively. The COF of pure PVE is also presented as 0.000 concentration in comparison to nanolubricants.

Even though the frictional test was conducted for a complete hour, the data are presented only from 1000 to 3600 s. During this period, the COF showed a consistent reading. In Figure 9a, the COF for  $\text{SiO}_2/\text{PVE}$  nanolubricants with the concentration of 0.003%, 0.005%, and 0.007% show lower values compared to the COF of pure PVE. Other samples showed higher COF. This trend indicates that nanolubricants below 0.007% concentration had better COF than that of the pure lubricant. A similar trend happened for  $\text{TiO}_2/\text{PVE}$  nanolubricants in Figure 9b with a small difference. The only  $\text{TiO}_2/\text{PVE}$  nanolubricant that had higher COF than that of pure lubricant was the one with a 0.03% concentration. Because of this, the tribological measurement for nanolubricants was stopped at 0.03% without further continuation. It was expected that the COF of more than this limit would become higher and would not contribute any significant results to the current study.

For a better understanding of the COF changes, the difference between nanolubricants and pure PVE was calculated and is presented in Figure 10. The COF of nanolubricants was normalized with the COF of pure PVE lubricant for all prepared samples. The COF of  $\text{SiO}_2/\text{PVE}$  nanolubricants shows an increment trend from 0.003% to 0.03% concentration. A linear trend is observed for the first four points before the gradient decreases until it reaches 18% higher than that for pure PVE for 0.03% concentration. The COF changes also illustrate that the  $\text{SiO}_2/\text{PVE}$  nanolubricant with low concentration (less than 0.007%) shows a decrement compared to that of the base lubricant. The COF trend of  $\text{TiO}_2/\text{PVE}$  has a slightly different trend. The first four concentrations show a decrement compared to that of base lubricant. However, the COF value is not linear. The nanolubricant with a concentration of 0.015% had the lowest COF. The linear COF increment appears from this point until it crosses the baseline at 0.03%.

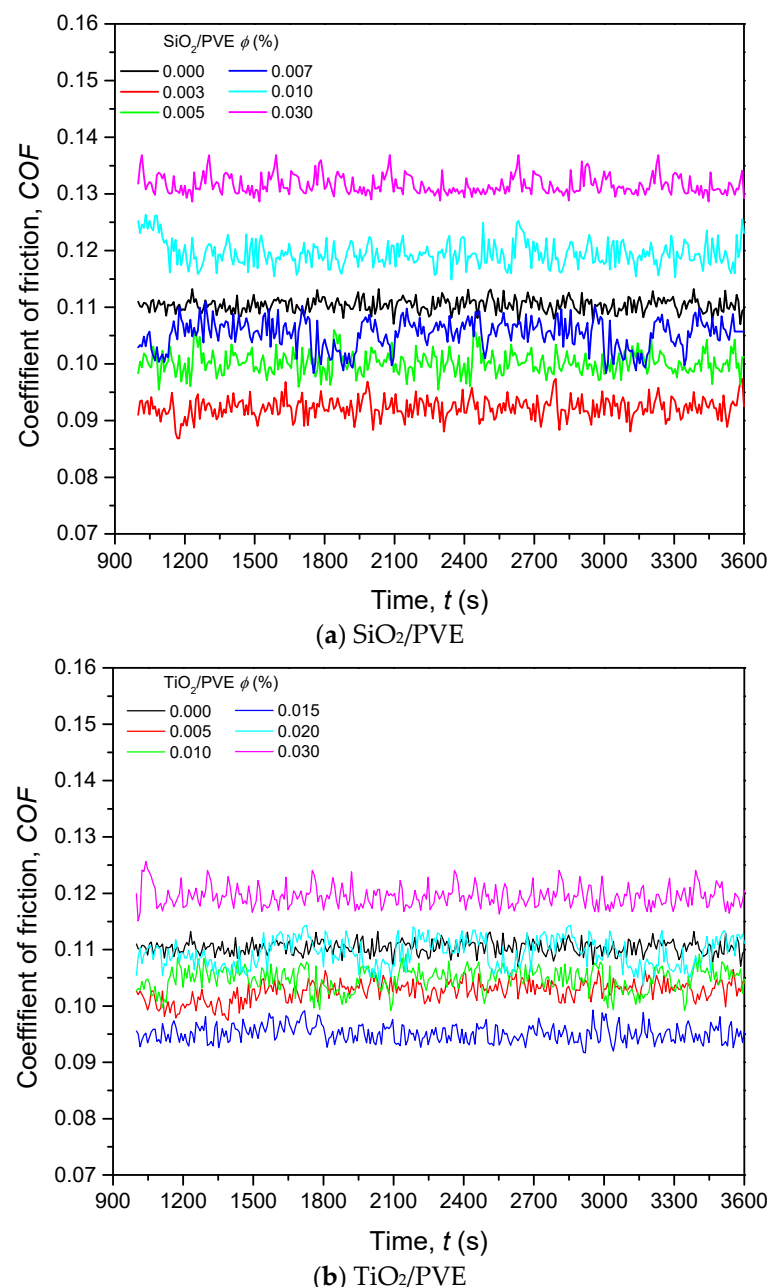


**Figure 9.** Coefficient of friction for nanolubricants in comparison to pure PVE lubricant.

The COF of nanolubricants was expected to decrease at low concentrations due to the small amount of nanoparticles present in the lubricant. The inclusion of a small amount of nanoparticles in nanolubricant may fill the gap produced by the wear effect between solid surfaces. Nanoparticles may create rolling and mending effects between surfaces together with the lubricant. However, there was a threshold for the usefulness of nanoparticles inside the lubricant. Exceeding this limit may result in the nanoparticle becoming abrasive against the contact surface. This has happened at a high concentration, i.e., 0.03%.

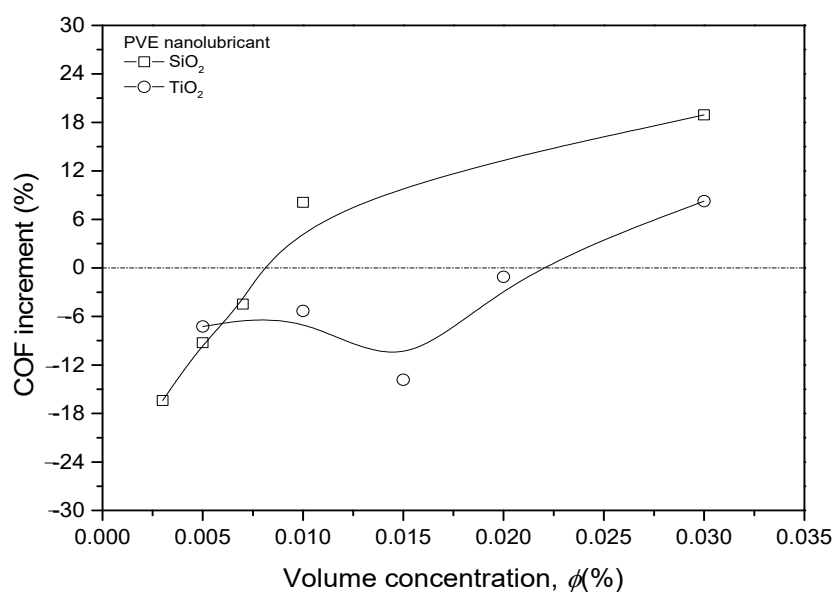


**Figure 10.** Nanolubricants coefficient of friction changes compared to PVE lubricant.

### 3.5. Wear Scar Analysis

The wear scar developed on the ball surfaces due to the rotational motion of the ball in the tribological experiment. A round scar formed on all three bottom balls, while a ring scar developed on the surface of the top ball. The size of WSD depends on the anti-wear capability of the lubricant as the surfaces were in contact. Smaller WSD indicate better lubrication performance due to the lower frictional effect acting on the ball surfaces. The WSD for each sample was inspected and measured just after completing the frictional test. The measurement recorded the radius, the area, and the perimeter of the wear scar of each stationary ball. The top ball had a circular line on its surface that was in contact with the three bottom balls. Figure 11 represents pictures captured of several wear scars on the surface of the balls.

Since the operating time for each lubricant was constant (3600 s), the size of the wear scar was solely affected by the anti-wear characteristics of the lubricant sample. A bigger WSD means that the lubricant sample has poor anti-wear characteristics and vice versa. The WSD for  $\text{SiO}_2/\text{PVE}$  0.003% has a smaller size than the 0.030% concentration. The same result goes for  $\text{TiO}_2/\text{PVE}$  nanolubricant with a concentration of 0.005% compared to 0.030%. The WSD for pure PVE was between these two concentrations. This WSD results in agreement with COF results in Figure 9. Nanolubricants with lower concentrations showed smaller WSD compared to those for higher concentrations.

The full results of WSD are presented in Figure 12. For comparison purposes, the WSD for nanolubricants were compared relative to WSD for pure PVE lubricant. The data in this figure show that wear scar sizes for nanolubricants with concentrations less than 0.010% and 0.020% for  $\text{SiO}_2/\text{PVE}$  and  $\text{TiO}_2/\text{PVE}$ , respectively, were smaller than the wear scar size for the base lubricant. Even the scar size became bigger when the concentration increased. For  $\text{SiO}_2/\text{PVE}$  nanolubricants, the sample with a concentration of 0.003% was the smallest, while for  $\text{TiO}_2/\text{PVE}$ , 0.015% was the smallest. The WSD trends were almost similar to the COF changes presented in Figure 10. The wear scar size supports the findings of COF, where the  $\text{SiO}_2$  and  $\text{TiO}_2$  nanoparticles behaved as anti-wear agents in lubricants at low volume concentrations. By the increment of concentration, the abrasive behavior of nanoparticles increased until the abrasive behavior had a higher impact than the anti-wear behavior, thus producing more disadvantages to the overall process. Because of this, it was suggested that the tribological measurements stop at concentrations of 0.030%.

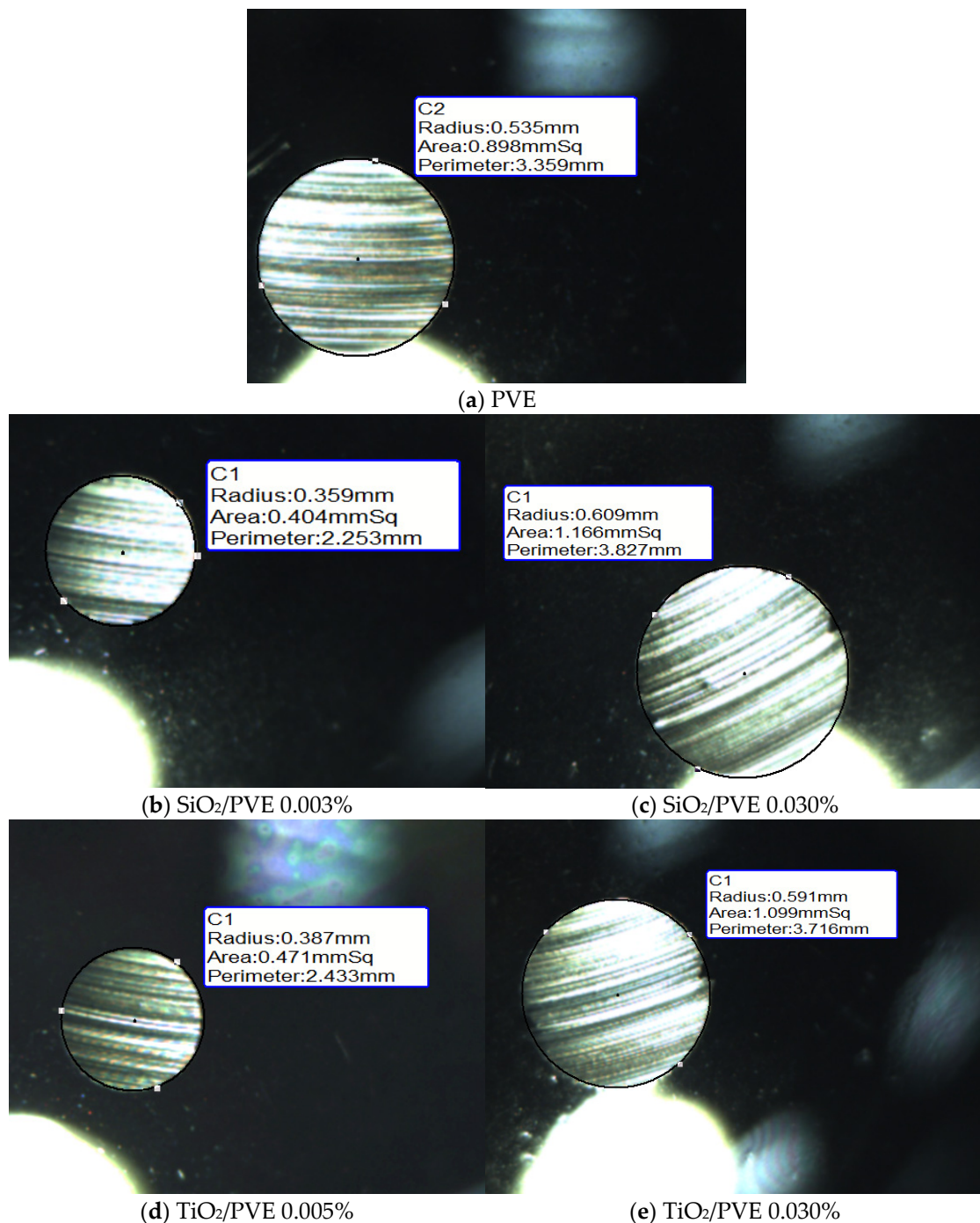


**Figure 11.** Regression model and statistical analysis of nanolubricants thermal conductivity.

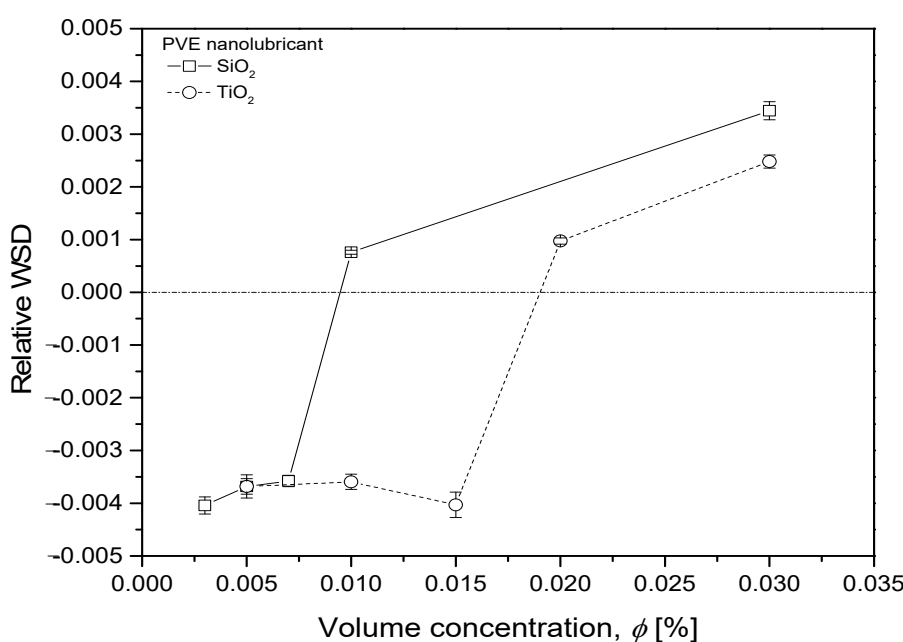


**Figure 12.** WSD changes relative to pure PVE lubricant for nanolubricants.

#### 4. Conclusions

The present paper focuses on the effect of thermal and tribological properties by nanoparticle dispersion in lubricant.  $\text{SiO}_2$  and  $\text{TiO}_2$  nanoparticles were dispersed homogeneously in PVE lubricant. Nanolubricants were characterized and their stability was evaluated. Thermal properties were investigated from 30 to 80 °C while tribological properties were studied employing the four-ball method. The thermal conductivity increases by the increment of nanoparticles concentration but decreases with temperature increment for both  $\text{SiO}_2/\text{PVE}$  and  $\text{TiO}_2/\text{PVE}$  nanolubricants. Very promising results were obtained from nanolubricants with the concentration of 0.005 vol.% and 0.015 vol.% for  $\text{SiO}_2/\text{PVE}$  and  $\text{TiO}_2/\text{PVE}$  respectively, with a significant COF reduction of around 15%. The friction reduction was the effect of contact area reduction by the nanoparticle's morphology acting on the surface of two mechanical components that were in contact. The study also identifies the threshold value of nanoparticles as an additive for  $\text{SiO}_2$  and  $\text{TiO}_2$ ; 0.010 vol.% and 0.020 vol.%, respectively; to exceed this may cause an increment in friction. The wear scar radius on the ball surface confirms the friction reduction effect by nanoparticles. The thermal conductivity regression model was also proposed for both types of nanolubricants with a high confidence level.  $\text{SiO}_2$  and  $\text{TiO}_2$  additives in nanolubricant improved the thermal and tribological properties of PVE oil with the condition that the nanoparticle concentration does not exceed the threshold value.

**Author Contributions:** Conceptualization, M.F.I. and W.H.A.; methodology, M.F.I.; validation, M.F.I., W.H.A. and R.M.; formal analysis, M.F.I.; investigation, M.F.I.; resources, W.H.A. and R.M.; data curation, W.H.A. and R.M.; writing—original draft preparation, M.F.I.; writing—review and editing, W.H.A. and H.M.A.; visualization, M.F.I.; supervision, W.H.A. and R.M.; project administration, W.H.A.; funding acquisition, R.M. and H.M.A. All authors have read and agreed to the published version of the manuscript.

**Funding:** This research was funded by the Universiti Malaysia Pahang under the International Publication Grant (RDU213302) and additional financial support under Postgraduate Research Grant (PGRS2003202).

**Institutional Review Board Statement:** Not applicable.

**Informed Consent Statement:** Not applicable.

**Data Availability Statement:** Not applicable.

**Acknowledgments:** The authors acknowledge the contributions of the research teams from the Center for Research in Advanced Fluid and Processes (Pusat Bendalir) and the Advanced Automotive Liquids Laboratory (AALL), who provided valuable insight and expertise for the current study.

**Conflicts of Interest:** The authors declare no conflict of interest.

## References

1. Kotia, A.; Rajkhowa, P.; Rao, G.S.; Ghosh, S.K. Thermophysical and tribological properties of nanolubricants: A review. *Heat Mass Transf.* **2018**, *54*, 3493–3508. [[CrossRef](#)]
2. Holmberg, K.; Erdemir, A. Influence of tribology on global energy consumption, costs and emissions. *Friction* **2017**, *5*, 263–284. [[CrossRef](#)]
3. Kamel, B.M.; El-Kashif, E.; Hoziefa, W.; Shiba, M.S.; Elshalakany, A. The effect of MWCNTs/GNs hybrid addition on the tribological and rheological properties of lubricating engine oil. *J. Dispers. Sci. Technol.* **2021**, *42*, 1811–1819. [[CrossRef](#)]
4. Exxon-Mobil. *2019 Outlook for Energy: A Perspective to 2040*; Exxon Mobil Corporation: Irving, TX, USA, 2019.
5. Sharif, M.Z.; Azmi, W.H.; Redhwan, A.A.M.; Mamat, R.; Najafi, G. Energy saving in automotive air conditioning system performance using SiO<sub>2</sub>/PAG nanolubricants. *J. Therm. Anal. Calorim.* **2019**, *135*, 1285–1297. [[CrossRef](#)]
6. Azmi, W.H.; Sharif, M.Z.; Yusof, T.M.; Mamat, R.; Redhwan, A.A.M. Potential of nanorefrigerant and nanolubricant on energy saving in refrigeration system—A review. *Renew. Sustain. Energy Rev.* **2017**, *69*, 415–428. [[CrossRef](#)]
7. Azmi, W.H.; Hamid, K.A.; Usri, N.A.; Mamat, R.; Sharma, K.V. Heat transfer augmentation of ethylene glycol: Water nanofluids and applications—A review. *Int. Commun. Heat Mass Transf.* **2016**, *75*, 13–23. [[CrossRef](#)]
8. Azmi, W.H.; Sharma, K.V.; Mamat, R.; Najafi, G.; Mohamad, M.S. The enhancement of effective thermal conductivity and effective dynamic viscosity of nanofluids—A review. *Renew. Sustain. Energy Rev.* **2016**, *53*, 1046–1058. [[CrossRef](#)]
9. Wang, R.; Hao, B.; Xie, G.; Li, H. A refrigerating-system using HFC134a and mineral lubricant appended with N-TiO<sub>2</sub> as working fluids. In Proceedings of the 4th International Symposium on Heating, Ventilating and Air Conditioning, Beijing, China, 9–11 October 2003; pp. 888–892.
10. Redhwan, A.A.M.; Azmi, W.H.; Sharif, M.Z.; Zawawi, N.N.M.; Zulkarnain, O.W.; Aminullah, A.R.M. The effect of Al<sub>2</sub>O<sub>3</sub>/PAG nanolubricant towards automotive air conditioning (AAC) power consumption. In Proceedings of the Symposium on Energy Systems 2019, Kuantan, Malaysia, 1–2 October 2019; p. 012056.
11. Yang, S.; Cui, X.; Zhou, Y.; Chen, C. Study on the effect of graphene nanosheets refrigerant oil on domestic refrigerator performance. *Int. J. Refrig.-Rev. Int. Froid* **2020**, *110*, 187–195. [[CrossRef](#)]
12. Saravanan, A.L.; Lal, D.M.; Selvam, C. Experimental Investigation on the Performance of Condenser for Charge Reduction of HC-290 in a Split Air-Conditioning System. *Heat Transf. Eng.* **2020**, *41*, 1499–1511. [[CrossRef](#)]
13. Sharif, M.Z.; Azmi, W.H.; Redhwan, A.A.M.; Mamat, R. Investigation of thermal conductivity and viscosity of Al<sub>2</sub>O<sub>3</sub>/PAG nanolubricant for application in automotive air conditioning system. *Int. J. Refrig.* **2016**, *70*, 93–102. [[CrossRef](#)]
14. Masuda, H.; Ebata, A.; Teramae, K.; Hishinuma, N. Alteration of thermal conductivity and viscosity of liquid by dispersing ultra-fine particles. Dispersion of Al<sub>2</sub>O<sub>3</sub>, SiO<sub>2</sub> and TiO<sub>2</sub> ultra-fine particles. *Netsu Bussei* **1993**, *7*, 227–233. [[CrossRef](#)]
15. Choi, S.U.S.; Eastman, J.A. Enhancing thermal conductivity of fluids with nanoparticles. In Proceedings of the ASME International Mechanical Engineering Congress & Exposition, San Francisco, CA, USA, 12–17 November 1995.
16. Nikitin, D.; Zhelezny, V.; Prihodchenko, N.; Ivchenko, D. Surface Tension, Viscosity, and Thermal Conductivity of Nanolubricants and Vapor Pressure of Refrigerant/Nanolubricant Mixtures. *Восточно-Европейский Журнал Передовых Технологий* **2011**, *5*, 12–17.
17. Ouikhalfan, M.; Labihi, A.; Belaqziz, M.; Chehouani, H.; Benhamou, B.; Sari, A.; Belfkira, A. Stability and thermal conductivity enhancement of aqueous nanofluid based on surfactant-modified TiO<sub>2</sub>. *J. Dispers. Sci. Technol.* **2020**, *41*, 374–382. [[CrossRef](#)]
18. Redhwan, A.A.M.; Azmi, W.H.; Sharif, M.Z.; Mamat, R.; Zawawi, N.N.M. Comparative study of thermo-physical properties of SiO<sub>2</sub> and Al<sub>2</sub>O<sub>3</sub> nanoparticles dispersed in PAG lubricant. *Appl. Therm. Eng.* **2017**, *116*, 823–832. [[CrossRef](#)]
19. Zawawi, N.N.M.; Azmi, W.H.; Redhwan, A.A.M.; Sharif, M.Z.; Sharma, K.V. Thermo-physical properties of Al<sub>2</sub>O<sub>3</sub>-SiO<sub>2</sub>/PAG composite nanolubricant for refrigeration system. *Int. J. Refrig.-Rev. Int. Froid* **2017**, *80*, 1–10. [[CrossRef](#)]
20. Marcucci Pico, D.F.; da Silva, L.R.R.; Hernandez Mendoza, O.S.; Bandarra Filho, E.P. Experimental study on thermal and tribological performance of diamond nanolubricants applied to a refrigeration system using R32. *Int. J. Heat Mass Transf.* **2020**, *152*, 119493. [[CrossRef](#)]
21. Kumar, R.S.; Narukulla, R.; Sharma, T. Comparative Effectiveness of Thermal Stability and Rheological Properties of Nanofluid of SiO<sub>2</sub>-TiO<sub>2</sub> Nanocomposites for Oil Field Applications. *Ind. Eng. Chem. Res.* **2020**, *59*, 15768–15783. [[CrossRef](#)]
22. Sanukrishna, S.S.; Shafi, M.; Murukan, M.; Jose Prakash, M. Effect of SiO<sub>2</sub> nanoparticles on the heat transfer characteristics of refrigerant and tribological behaviour of lubricant. *Powder Technol.* **2019**, *356*, 39–49. [[CrossRef](#)]
23. Sanukrishna, S.S.; Krishnakumar, T.S.; Vishnu, S.; Jose Prakash, M. Effect of oxide nanoparticles on the thermal, rheological and tribological behaviours of refrigerant compressor oil: An experimental investigation. *Int. J. Refrig.* **2018**, *90*, 32–45. [[CrossRef](#)]
24. Zawawi, N.N.M.; Azmi, W.H.; Sharif, M.Z.; Shaiful, A.I.M. Composite nanolubricants in automotive air conditioning system: An investigation on its performance. In Proceedings of the 1st International Postgraduate Conference on Mechanical Engineering, Pekan, Malaysia, 31 October 2018; p. 012078.

25. Zin, V.; Barison, S.; Agresti, F.; Colla, L.; Pagura, C.; Fabrizio, M. Improved tribological and thermal properties of lubricants by graphene based nano-additives. *RSC Adv.* **2016**, *6*, 59477–59486. [CrossRef]
26. Idemitsu Kosan Co., Ltd. Characteristics of Daphne Hermetic Oil. Available online: [www.idemitsu.com/business/lube/pve/daphne.html](http://www.idemitsu.com/business/lube/pve/daphne.html) (accessed on 1 January 2020).
27. Motozawa, M.; Makida, N.; Fukuta, M. Experimental Study on Physical Properties of CuO—PVE Nano-oil and its Mixture with Refrigerant. In Proceedings of the International Compressor Engineering Conference, West Lafayette, IN, USA, 9–12 July 2018.
28. Matsumoto, T.; Kaneko, M.; Tamano, M. Properties of Polyvinylether (PVE) as a Lubricant for Air Conditioning systems with HFC Refrigerants? Data Update? In Proceedings of the International Refrigeration and Air Conditioning Conference, West Lafayette, IN, USA, 12–15 July 2010; pp. 1–8.
29. Ismail, M.F.; Azmi, W.H.; Mamat, R.; Rahim, R.A. Rheological Behaviour and Thermal Conductivity of Polyvinyl Ether Lubricant Modified with SiO<sub>2</sub>-TiO<sub>2</sub> Nanoparticles for Refrigeration System. *Int. J. Refrig.* **2022**, *138*, 118–132. [CrossRef]
30. Ismail, M.F.; Wan Hamzah, W.A. Tribological Performance Effect of SiO<sub>2</sub> and TiO<sub>2</sub> Nanoparticles as Lubricating Oil Additives. In Proceedings of the 2nd Energy Security and Chemical Engineering Congress; Springer: Singapore, 2023; pp. 223–231.
31. Hamisa, A.H.; Azmi, W.H.; Yusof, T.M.; Ismail, M.F.; Ramadhan, A.I. Rheological Properties of TiO<sub>2</sub>/POE Nanolubricant for Automotive Air-Conditioning System. *J. Adv. Res. Fluid Mech. Therm. Sci.* **2021**, *90*, 10–22. [CrossRef]
32. Sharif, M.Z.; Azmi, W.H.; Zawawi, N.N.M.; Ghazali, M.F. Comparative air conditioning performance using SiO<sub>2</sub> and Al<sub>2</sub>O<sub>3</sub> nanolubricants operating with Hydrofluoroolefin-1234yf refrigerant. *Appl. Therm. Eng.* **2022**, *205*, 118053. [CrossRef]
33. Sharif, M.Z.; Azmi, W.H.; Redhwan, A.A.M.; Zawawi, N.N.M. Preparation and stability of silicone dioxide dispersed in polyalkylene glycol based nanolubricants. In Proceedings of the MATEC Web of Conferences, Cyberjaya, Malaysia, 2–3 August 2016; p. 01049.
34. Mostafizur, R.M.; Aziz, A.R.A.; Saidur, R.; Bhuiyan, M.H.U. Investigation on stability and viscosity of SiO<sub>2</sub>-CH<sub>3</sub>OH (methanol) nanofluids. *Int. Commun. Heat Mass Transf.* **2016**, *72*, 16–22. [CrossRef]
35. Hongwu International Group Ltd. Anatase Nano TiO<sub>2</sub> Titanium Dioxide Powders. Available online: [www.hwnanomaterial.com/anatase-nano-tio2-titanium-dioxide-powders\\_p49.html](http://www.hwnanomaterial.com/anatase-nano-tio2-titanium-dioxide-powders_p49.html) (accessed on 25 September 2021).
36. Beijing Deke Daojin Science and Technology Co., Ltd. Nano Silica. Available online: [www.dknano.com/EcpLB.asp?Fid=1177&ClassId=1190&NewsId=2993](http://www.dknano.com/EcpLB.asp?Fid=1177&ClassId=1190&NewsId=2993) (accessed on 25 September 2021).
37. Hamilton, R.L.; Crosser, O.K. Thermal conductivity of heterogeneous two-component systems. *Ind. Eng. Chem. Fundam.* **1962**, *1*, 187–191. [CrossRef]
38. Wang, H.; Wang, Y.M. Tribological Performance of AlN nanoparticles as lubricating oil additive. *Adv. Mater. Res.* **2012**, *366*, 238–242. [CrossRef]
39. Sanukrishna, S.S.; Vishnu, A.S.; Jose, M. Nanorefrigerants for energy efficient refrigeration systems. *J. Mech. Sci. Technol.* **2017**, *31*, 3993–4001. [CrossRef]
40. Qing, S.H.; Rashmi, W.; Khalid, M.; Gupta, T.; Nabipoor, M.; Hajibeigy, M.T. Thermal conductivity and electrical properties of hybrid SiO<sub>2</sub>-graphene naphthenic mineral oil nanofluid as potential transformer oil. *Mater. Res. Express* **2017**, *4*, 015504. [CrossRef]
41. Al-Janabi, A.S.; Hussin, M.; Jaafar, M.; Sharif, N.M. Stability and thermal conductivity of graphene in polyester nanolubricant. *AIP Conf. Proc.* **2020**, *2267*, 020066.
42. Ghadimi, A.; Saidur, R.; Metselaar, H.S.C. A review of nanofluid stability properties and characterization in stationary conditions. *Int. J. Heat Mass Transf.* **2011**, *54*, 4051–4068. [CrossRef]

**Disclaimer/Publisher’s Note:** The statements, opinions and data contained in all publications are solely those of the individual author(s) and contributor(s) and not of MDPI and/or the editor(s). MDPI and/or the editor(s) disclaim responsibility for any injury to people or property resulting from any ideas, methods, instructions or products referred to in the content.